INL/JOU-25-84347-Revision-0

Effect of Particle size and moisture on flow performance of loblolly pine anatomical fractions: Experimental findings and model predictions

October 2025

Changing the World's Energy Future

Nepu Saha, Jordan Lee Klinger, Tiasha Bhattacharjee, Noah James Berglund, Wencheng Jin, Yidong Xia

Idaho National Laboratory

INL/JOU-25-84347-Revision-0

Effect of Particle size and moisture on flow performance of loblolly pine anatomical fractions: Experimental findings and model predictions

Nepu Saha, Jordan Lee Klinger, Tiasha Bhattacharjee, Noah James Berglund, Wencheng Jin, Yidong Xia

October 2025

Idaho National Laboratory
Idaho Falls, Idaho 83415

http://www.inl.gov

Prepared for the
U.S. Department of Energy
Under DOE Idaho Operations Office
Contract DE-AC07-05ID14517, DE-AC07-05ID14517, DE-AC07-05ID14517

Effect of Particle size and moisture on flow performance of loblolly pine anatomical fractions: Experimental findings and model predictions

Nepu Saha[1*], Jordan Klinger[1], Tiasha Bhattacharjee[1], Noah Berglund[1], Wencheng Jin[1,2], Yidong Xia[1],

[1]Energy and Environment Science & Technology Directorate, Idaho National Laboratory, Idaho Falls, ID 83415, USA

[2]Harold Vance Department of Petroleum Engineering, Texas A&M University, College Station, TX 77843, USA

* Corresponding Author: Email: nepu.saha@inl.gov, Tel: +1 208 526 4702

Graphical Abstract

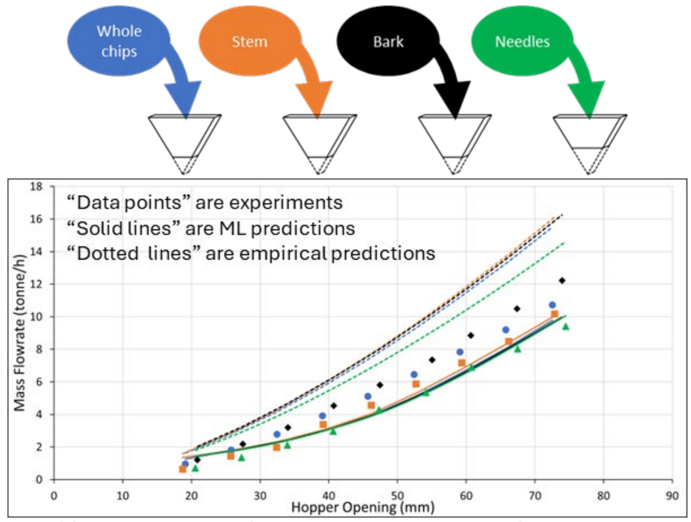

Empirical models overestimate and respond to woody tissue, whereas ML methods achieve central tendency but lack tissue type discrimination.

Abstract

The rising energy demand has highlighted biomass as a promising next-generation energy source. However, commercializing biomass-derived energy faces challenges, particularly in handling biomass feedstock. Factors like particle size, shape, moisture content, and surface roughness significantly impact biomass flowability. This study addresses a crucial knowledge gap by examining the effects of particle size and moisture content on the flow behavior and shear properties of different anatomical fractions of loblolly pine (*Pinus taeda*). The bulk shear behavior was examined using a Schulze ring shear tester, while flow performance was tested through gravity-driven flow experiments in a variable wedge-shape hopper. Results were incorporated into empirical and machine learning-based flow prediction models to evaluate their accuracy and limitations. The study found that samples with higher moisture content show higher unconfined yield strength. The critical arching distance increased with particle size, *e.g.*, from approximately 13 and 33 mm for 2- and 6-mm whole chips, respectively at a 32-degree inclination angle. Conversely, the flow rate decreased for a given hopper opening as particle size increased. For instance, at a 60-mm hopper opening and a 32-degree inclination angle, the mass flow rates for 2- and 6-mm whole chips were 7.83 and 6.42 tonne/h, respectively. The empirical model consistently overpredicted the mass flow rate for all anatomical fractions, while the machine learning model more accurately predicted the central tendency of flow rate but was insensitive to varying tissue proportions. These novel findings provide comprehensive characterization of anatomical fractions, reveal significant combined effects of particle size and moisture content on biomass flow behavior, and demonstrate a better predictive accuracy of a machine learning model, all of which are useful for optimizing material handling strategies and biomass utilization technologies in the industry.

Keywords: Biomass; anatomical fractions; material handling; flowability; flow model.

Highlights:

- Study examines particle size and moisture effects on loblolly pine residues flow.
- Arching distances were 13 and 33 mm for 2 and 6 mm chips, respectively at a 32° IA.
- Empirical model overpredicted flow rates, showing limitations for biomass fractions.
- ML model predicted flow rates with RMSE of 0.37-0.53 tonne/h.

1 Introduction

The escalating demand for alternative energy sources is driving efforts to achieve energy independence in the United States. Owing to its abundance and accessibility, biomass exhibits substantial potential to serve as a pivotal alternative energy source. However, the successful commercialization of biomass as an energy source faces challenges, particularly in the handling of biomass feedstock. Various factors, such as particle size, shape, moisture content, and surface roughness, influence the flow properties of biomass materials [1-3]. Inadequate understanding of biomass flowability during feedstock conversion process design can lead to process downtime caused by issues like feed silo ratholing and screw feeder jamming [4-9].

Historically, bulk solid flow studies were focused mainly on isotropic solids such as pharmaceutical ingredients and food powders with regular, uniform particle shapes and sizes at minimal moisture content [10-14]. However, biomass particles exhibit unique characteristics, including high moisture content, hygroscopic nature, low bulk density, heterogeneous shapes, and fibrous nature, which make them distinct from the conventional bulk solids [15, 16]. These characteristics pose challenges in experimentally measuring the flow properties of biomass particles. A comprehensive understanding of biomass flow behavior based on intrinsic material properties is essential to minimize downtime and improve the feasibility of feedstock conversion processes.

Loblolly pine (*Pinus taeda*) is one of the most widely planted and economically important pine species in the southeastern United States [17, 18]. Its consistent growth and availability make it an attractive candidate for various biofuel and biochemical applications. Research in the Feedstock-Conversion Interface Consortium (FCIC) supported by the U.S. Department of Energy has focused on loblolly pine to understand the critical material attributes on the operational reliability of biorefineries. Loblolly pine consists of distinct anatomical fractions, including whole chips, stem wood, bark, and needles, each exhibiting unique physical properties. The behavior of these anatomical fractions under different flow conditions remains relatively unexplored, limiting the optimization of handling processes and overall efficiency. Recently, Navar *et al.* [19] investigated the influence of moisture content on the rheological properties of various anatomical fractions of loblolly pine. Their findings revealed that certain anatomical fractions, such as bark and needle, exhibited a direct correlation between moisture content and rheological properties. However, no discernible influence of moisture content was observed for other fractions, including stem and whole. Interestingly, the impact of moisture content on the rheological properties was only evident for smaller particle sizes of bark and needle with a nominal size of 2 mm, while no significant effects were observed for larger particle sizes with a nominal size of 4 mm across the four anatomical fractions studied. The study examines the influence of moisture content on various anatomical fractions; it largely confirms known trends such as increased moisture leading to higher cohesion, without providing deeper mechanistic understandings of these relationships. Unfortunately, no experimental investigation on the impact of moisture content and particle size of various anatomical fractions was conducted. The efficient handling and utilization of biomass feedstocks are critical for optimizing industrial processes and achieving long-term production goals. In this context, the flow behavior and shear properties of particulate materials play a pivotal role in ensuring smooth and reliable processing. Particle size distribution and moisture content are key factors influencing the flow characteristics of bulk solids as Navar *et al.* [19] recently found their effect on rheological properties. Understanding their combined effects on different anatomical fractions of loblolly pine is essential for improving the design and operation of biomass processing systems. In addition to the experimental investigation of flow performance, accurate prediction and precise control of hopper throughput are crucial for trouble-free operation. Numerous numerical flow models exist for conventional granular materials (*e.g.,* pharmaceutical particles, rocks, coal, and ores) [20-24]. However, biomass exhibits significantly different behavior compared to those materials [25]. Lu *et al.* [26] examined the influence of critical material attributes of biomass (*e.g.,* loblolly pine, Douglas fir) on flow pattern, arching, and throughput using both experimental method and numerical simulation. Their findings indicate that flow throughput can be estimated using an empirical equation that incorporates inputs on hopper geometry (*e.g.,* hopper outlet size) and material attributes at particle and bulk scales. A recent study by the same group, Ikbarieh *et al.* [27], introduced a machine learning (ML) based approach to predict the flow performance of loblolly pine. Their results demonstrated promising predictive accuracy, revealing that hopper opening width primarily dictates flow throughput, while relative density, wall friction, inclination angle, and hopper opening width collectively influence flow stability. It is worth noting that none of these studies attempted to predict the flow performance of the anatomical fractions of biomass, leaving this an unexplored research area that warrants the need for further investigation.

This present study aims to address the critical knowledge gap regarding the effect of particle size and moisture content on the flow behavior and shear properties of different anatomical fractions of loblolly pine. We conducted a comprehensive investigation into the physical properties, including particle size distribution and bulk density, of different anatomical fractions of loblolly pine. Furthermore, the bulk shear behavior, encompassing the determination of apparent internal friction angle, bulk cohesion, and factors contributing to particle-particle friction, was explored using a Schulze ring shear tester. Additionally, this study examined how material attributes influenced flow performance through gravity-driven flow experiments using a variable wedge.

Subsequently, the obtained physical and shear properties were plugged into our recently developed flow prediction models, i) the empirical model [26], ii) the ML model [27], to predict the flow performance of the studied material. Finally, we discussed the applicability and limitations of the existing flow models considering the experimental results. By providing comprehensive data and analysis, this research will contribute significantly to advancing biomass utilization technologies.

2 Material and Methods

2.1 Material

Loblolly pine (*Pinus taeda*) was collected from a plantation in Jasper County of South Carolina where a logging operation was used to harvest the bole of the trees. The trees were 18 years old and averaged 61 feet in height. The tree limbs, tops, bark and needles were piled on the ground and are considered as residues from the lumber harvest. These residues accumulated during the harvest for about 2 weeks and then picked up in scoops by grapple front end loader and were processed through a horizontal grinder (Peterson Horizontal grinder Model 4710B). The size reduced samples were fed by a rubber conveyor into a covered truck for transport to Idaho National Laboratory (INL) facility. After arriving at the facility, some of the residues were processed with an air separator (Spudnik Air-Sep, Spudnik Equipment Co, Blackfoot, Idaho, USA) to obtain fractions that were enriched in either bark, needles, or white wood compared to the whole residues to examine their impact on flow performance. The samples were then size reduced using a low RPM shredder (Crumbler® M24, Forest Concepts, Auburn, Washington, USA) with rotor heads of nominally 2, 4, and 6mm sizes. This is a continuous milling device that passes material through a set of 2 interlocked rotor heads that are sized to a nominal 2, 4, and 6mm respective cutting disc thickness. During operations, the rotor rotational frequency is approximately 300/min. The overall feed rate was 100-250 kg/h depending on size and sample. No vacuum assistance was used during size reduction. Figure 1 shows the material of different sizes and anatomical fractions used in this study.

Figure 1: Different sizes and anatomical fractions of loblolly pine.

2.2 Methods

2.2.1 Physical properties

Moisture content was measured following the American Society of Agricultural and Biological Engineers (ASABE) standard S358.2 [28]. In summary, this involved placing a 50–100 g sample in a horizontal convective oven at 105 °C for 24–30 hours. The mass loss of the samples, assumed to be primarily moisture, was reported on a wet basis using the following equation:

$$MC = \frac{m_{wet} - m_{dry}}{m_{wet}} \times 100\%$$

Where MC represents the percent moisture content of the sample (on a wet mass basis), m_{wet} is the mass of the sample before drying, and m_{dry} is the mass of the sample after drying.

Particle size distribution (PSD) analysis was conducted using a standard Ro-Tap separator (Model RX-29) by following the ASAE S319.3 standard [29]. The procedure involved loading the sample into the top sieve, assembling the sieve stack in the Ro-Tap machine, and activating the separator for a duration of ten minutes. During this process, the Ro-Tap separator tapped and rotated the sieves, causing the particles to pass through the sieves until they reached a mesh smaller than their characteristic size. After the ten-minute run, the sieve stack was disassembled, and each sieve was weighed. By subtracting the tare weights for each sieve, the relative amount of each sample passing through each successive sieve was determined. Cumulative particle passing distributions (CPDs) were then calculated based on these measured weights. The 50% cumulative passing percentile sieve size (D_{50}) was determined by linear interpolation to find the theoretical sieve size corresponding to retaining 50% of the particles by mass. Likewise, the 10% and 90% cumulative passing (D_{10} and D_{90}, respectively) were also calculated and reported based on the CPDs obtained from the analysis.

The bulk density (BD) and tapped density (TD) of the tested samples were determined using a modified version of the ASAE standard method S269.4 [30]. In the BD measurement process, a sample of the material was poured into a graduated cylindrical container with a diameter of 120 mm. The sample was poured from a height of 0.6 m above the container's top edge to ensure uniform settling. The pouring continued until the height of the material in the container reached approximately 90% of the container's diameter. To estimate the BD of the sample, the volume was calculated based on the average sample height, determined by taking four measurements at different locations within the container. Finally, the mass of the sample was divided by the average volume to obtain the BD value. After measuring the BD, the container containing the sample was subjected to five drops from a height of 0.15 m onto a hard surface, as per the standard tapping procedure. This tapping process aimed to settle the particles and achieve a more compact arrangement in the container. Following the tapping process, the TD was estimated using the same methodology used for the BD measurement described earlier.

The envelope density, referred to as particle density (PD) in this study, was measured using a Geopyc 1365 (Micromeritics, Norcross, GA). Detailed experimental procedures are available elsewhere [31]. Briefly, a known volume of DryFlo® granular medium was added to a cylindrical chamber with a biomass sample of known mass. The DryFlo® granular medium was consolidated around the sample by rotating and vibrating the cylindrical chamber while a piston gradually compressed the chamber until the desired force was achieved. This was followed by retraction and recompression. Pores open to the particle exterior but smaller than the DryFlo® particles were included within the volume. The sample volume was determined by subtracting the volume of the DryFlo®. The PD was then calculated by dividing the sample mass by the sample volume.

2.2.2 Shear properties

A Schulze rotary shear tester was used to perform shear tests (ASTM standard methods) and generate yield loci of the various anatomical fractions at different sizes. In the test setup, an annular shear cell is loaded with the sample and a veined lid (veins provide no-slip boundaries at top and bottom surfaces) is placed on top of the cell. The lid is then connected to an adjustable counterweight system with the help of two tie rods. A normal compressive stress (pre-shear stress) is applied to the lid, with a weighted counter lever. The bottom ring rotates relative to the fixed lid at approximately 0.01 rad/s and the shear forces generated in the bulk material are obtained from the measured rotational torque in the tie rods. After reaching target pre-shear stress (1kPa), the material is sheared at 3 different stress (100, 250, 700 Pa), with unloading and relaxation before each pre-shear step, to generate the yield loci. The yield locus of the material is developed as a function of the shear and compressive stresses. Mechanical properties of the bulk material including bulk cohesion, unconfined yield strength, major principal stress and internal angle of friction are obtained from the yield loci.

2.2.3 Flow performance

To investigate and elucidate the impact of variable material attributes on flow performance in real flow systems, a comprehensive analysis was conducted utilizing the wedge hopper. Specifically designed for these tests, a custom hopper with adjustable outlet and sidewalls was employed to measure the critical arching distance and flow rate of the studied feedstocks. The custom hopper comprised two sidewalls and two vertical end walls. For the critical arching distance and flow tests, approximately 15 kg of each sample was loaded into the adjustable hopper for each batch test. The inclination angle of the sidewalls systematically varied between 28 to 36° at 4° intervals, while the end walls remained fixed at a distance of 400 mm throughout all tests. The hopper opening was incrementally increased using 2-step motors attached to the sidewalls. Figure 2 shows the adjustable hopper outlets and sidewalls used for flow testing, along with schematic and dimensions. The minimum opening required for all the loaded material to smoothly flow out from the hopper was defined as the critical arching distance of the material. This critical arching distance was determined for each sample at each inclination angle. Subsequently, the flow test was conducted at nine random openings beyond the critical arching distance of the hopper. The time taken for all the material to pass through the hopper opening was recorded, serving as the basis for flow rate calculation.

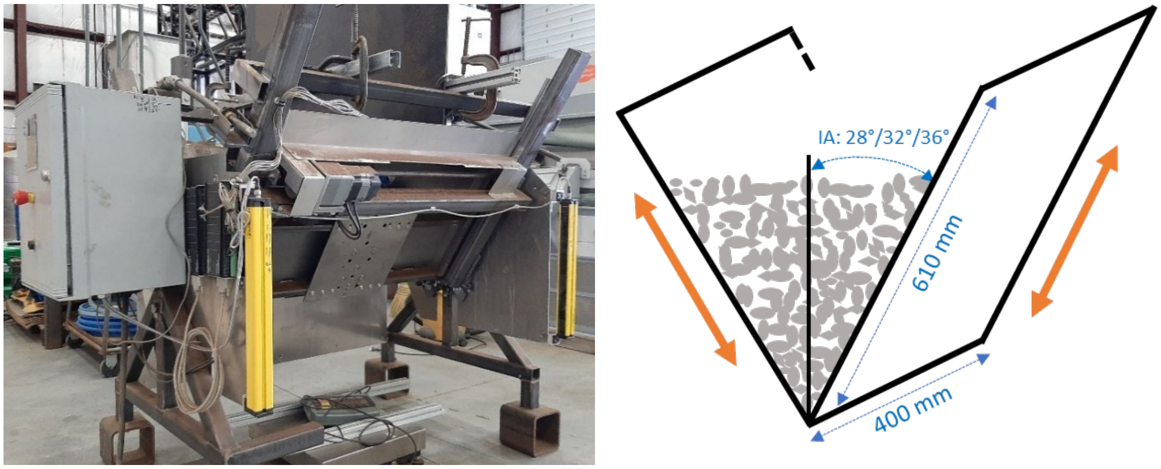

Figure 2: Lab scale adjustable hopper (left) and it's schematic (right).

Two different models were employed in this study to predict the mass flow rate of the hopper: (i) the empirical model [26] modified from the British Material Handling Board [32, 33]and (ii) a ML model [27]. The empirical model was calibrated based on experimental flow data and FEM (finite element method) numerical simulation flow data of whole loblolly pine samples and validated against experimental flow data of Douglas Fir. The model predicts mass flow rate (q_m) from the length (L), width (W), and wall friction (μ) of wedge-shaped hopper and material particle density (ρ_p), mean particle size (d_{50}), and bulk internal friction angle (ϕ_c) [26], as shown below:

$$q_m = a\rho_p\sqrt{g}\,(L - kd_{50})(W - kd_{50})^{1.5}\tan^{\mathrm{b}}\mu\tan^{c}\phi_c,$$

where a, b, c are fitting coefficients for different materials, g stands for gravity, while $k = 2.5$ is a constant and the kd_{50} term is used to account for effective outlet size width and length.

The ML model with a multilayer perceptron was trained using SPH (smoothed particle hydrodynamics) simulation data and validated against experimental flow data of whole loblolly pine with different moisture contents and mean particle sizes. The ML model consists of an input layer incorporating particles and bulk-scale attributes (*i. e.,* moisture content, mean particle size, relative density) and unit operation parameters (*i.e.,* inclination angle, wall friction, hopper opening width), as well as an output layer predicting mass flow rate (q_m) and flow pattern (*i.e.,* normalized average flow velocity at the middle of hopper). The input and output layers are connected by three hidden layers, which contain 1000, 750, and 300 neurons respectively and all used Leaky Relu activation functions. The number of hidden layers and neurons was chosen to promote model generalization and prevent the risk of both overfitting and underfitting.

The constitutive law of FEM simulations adopts a G–B hypoplastic model incorporating the critical state theory, and its three groups of material parameters, including shear properties (*e.g.,* internal friction angle), compression properties (*e.g.,* granulate hardness), and the range of void ratios, were calibrated against the experimental characterization (*e.g.,* Schulze ring shear, uniaxial compression) [34]. For the SPH simulations, the G-B constitutive law was enhanced to capture the significant interlock effects of biomass materials and adopted for the simulation. The empirical equation was formulated using both FEM simulation and experimental datasets, whereas the ML model was trained and tested exclusively on the SPH simulation dataset (*i.e.,* 2025 combinations of input variables). Notably, the SPH code and associated material parameters were calibrated against experimental flow data obtained from nine whole pine samples with varying moisture contents and mean particle sizes. Detailed information on the enhancement and the ML model can also be found elsewhere [27].

3 Results and Discussions

3.1 Physical properties

Table 1 presents data pertaining to the PSD and density of whole pine, alongside its anatomical fractions. Note that PSD of each sample was measured at least in triplicate to ensure the statistical significance. The observations indicate that both whole chips and stem wood exhibit comparable trends in PSD, which could be due to the predominant component in the whole chips begin the stem wood. Specifically, the D_{10}, D_{50}, and D_{90} parameters increase with an increase in nominal particle size. For instance, the D_{50} value for whole chips with a nominal size of 2 mm measures 1.51 mm, whereas it increases to 2.65 mm and 5.21 mm for nominal sizes of 4 mm and 6 mm, respectively. A similar trend was also observed for the stem and bark, but the needles demonstrate a distinct pattern. For instance, the D_{50} of 2 mm needles was 1.11 mm, whereas it was 1.76 mm and 1.73 mm for 4 mm and 6 mm needles, respectively. This discrepancy can be attributed to the distinctive shape (*e.g.,* lower, and limited effective diameter which allows to pass through the smaller sieve) of the needles in comparison to the other anatomical fractions.

Table 1: Physical properties of whole loblolly pine along with the anatomical fractions

Sample	Size (mm)	PSD (mm)			BD (kg/m^3)	TD (kg/m^3)	PD (kg/m^3)
		D_{10}	D_{50}	D_{90}			
Whole	2	0.91 ± 0.07	1.51 ± 0.07	2.49 ± 0.03	128.9 ± 3.9	144.6 ± 2.3	DNM*
	4	1.77 ± 0.03	2.65 ± 0.07	3.96 ± 0.16	125.0 ± 2.5	135.7 ± 6.0	463.0
	6	3.33 ± 0.01	5.21 ± 0.06	8.15 ± 0.22	120.0 ± 4.8	127.5 ± 7.0	DNM*
Stem	2	1.05 ± 0.05	1.58 ± 0.04	2.38 ± 0.02	131.1 ± 1.4	150.1 ± 4.9	DNM*
	4	2.58 ± 0.12	3.95 ± 0.04	6.06 ± 0.20	130.7 ± 2.3	139.4 ± 2.6	470.7
	6	3.59 ± 0.63	5.66 ± 0.58	8.91 ± 0.29	125.3 ± 2.5	136.0 ± 2.9	DNM*
Bark	2	0.70 ± 0.08	1.29 ± 0.09	2.36 ± 0.05	134.4 ± 9.3	150.9 ± 10.3	DNM*
	4	2.01 ± 0.05	3.25 ± 0.06	5.25 ± 0.05	132.2 ± 5.3	142.9 ± 4.8	452.0
	6	2.06 ± 0.23	3.84 ± 0.38	7.16 ± 0.63	99.3 ± 8.2	106.3 ± 13.8	DNM*
Needles	2	0.67 ± 0.08	1.11 ± 0.15	1.84 ± 0.28	127.0 ± 3.0	144.8 ± 7.3	DNM*
	4	0.90 ± 0.25	1.76 ± 0.28	3.42 ± 0.28	78.8 ± 16.6	92.3 ± 19.1	380.7
	6	0.85 ± 0.15	1.73 ± 0.24	3.55 ± 0.39	69.1 ± 8.6	79.0 ± 11.2	DNM*

* did not measure

Both bulk and tapped densities exhibit decreasing trends with increasing particle size. This observation aligns with existing literature, specifically Zamora-Cristales *et al.* [35], who reported a decrease in the bulk density of forest residues with larger nominal particle sizes resulting from two distinct comminution methods (*i.e.,* hammer mill and knife mill). Additionally, Zhu *et al.* [36]

demonstrated that plantation density significantly affects wood density and anatomical properties, which could influence the PSD and density trends observed in this study. Furthermore, Fernandes *et al.* [37] highlighted the variability in wood density and its dependence on anatomical and environmental factors, supporting the observed trends in this study.

Notably, the density of 2 mm needles was within the same order of magnitude as other anatomical fractions. However, 4 mm and 6 mm needles exhibited significantly lower densities. This phenomenon can be attributed to the high aspect ratio of the 4 mm and 6 mm needles, which do not pack efficiently, thereby leaving substantial void spaces and resulting in significantly reduced densities. Conversely, the aspect ratio of the 2 mm needles was sufficiently small to allow for more efficient packing, thus exhibiting higher density.

Furthermore, Table 1 indicates that the stem exhibits the highest PD, whereas the needles have the lowest PD. On the other hand, the PD of the whole material and bark was measured to be between that of the stem and needles, as expected. It is important to note that this study measured the PD of all anatomical fractions at a single particle size and assumed that PD remains constant across different size variations. This assumption is supported by Zhu *et al.* [36] and Fernandes *et al.* [37], who highlighted the variability in wood density and its dependence on anatomical and environmental factors.

3.2 Shear properties

Shear tests on biomass are important for determining its mechanical properties, such as shear strength, internal friction, and bulk cohesion. These properties are critical for optimizing processing and handling procedures, ensuring efficient operation of biomass handling, storage, and processing equipment [38, 39].

A design of experiments (DOE) was conducted using JMP statistical software to investigate the main effects of tissue type, particle size and moisture content. The primary properties of interest from these tests are unconfined yield strength (UYS), internal friction and bulk cohesion. UYS is a descriptive property of granular materials, representing the major principal stress required to cause shear failure in an unsupported bulk material based on its stress history [40]. The results shown in Table 2 indicates that the whole unfractionated residues and the bark fractions have slightly higher UYS than the other materials. Additionally, samples with higher moisture content show increased UYS. This is hypothesized to be attributed to the fact that bark and whole residues have more angular particles along with high surface roughness which promote interlocking and require more stress to yield under confinement [41]. Furthermore, wet particles exhibit increased adhesion due to capillary forces, contributing to higher UYS in the samples with higher moisture content [42].

Internal friction, influenced by material surface roughness and particle morphology, was found to be higher in the bark and whole fractions. This is thought to be due to their greater surface roughness. Generally, the internal friction increased with particle size, while moisture content had a modest, mostly decreasing effect. For the samples studied, bulk cohesion decreased with increasing particle size and increased with increasing moisture content. Bark samples exhibited the highest cohesion, followed by whole material, with stem showing the lowest values. Needles displayed inconsistent results for bulk cohesion, with the smallest size having low values and the largest size showing high values, likely due to the long aspect ratio of 6 mm particles [38]. These findings generally align with more exhaustive studies of the impact of particle size and shape present in the literature [44]. While initial tests identified the main effects, DOE augmentations suggested that additional testing with 2mm needles and 6mm stem samples at varying moisture level would be valuable for further exploring the implications of biomass tissue mixtures on shear properties.

Table 2: Effect of tissue type, particle size, and moisture content on the shear properties under 1kPa pre-shear condition.

Material	Size (mm)	Moisture content (%)	Major Principal Stress (kPa)	Unconfined Yield Strength (kPa)	Effective angle of friction (°)	Angle of internal friction (°)	Bulk cohesion (kPa)
Whole	2	5	2.40 ± 0.02	0.41 ± 0.05	46.97 ± 0.85	43.27 ± 0.89	0.09 ± 0.01
	2	40	2.31 ± 0.06	0.42 ± 0.06	45.20 ± 0.51	41.17 ± 0.81	0.09 ± 0.01
	6	40	2.17 ± 0.14	0.25 ± 0.13	46.86 ± 2.15	44.46 ± 3.40	0.05 ± 0.03
Stem	2	5	2.37 ± 0.16	0.28 ± 0.07	43.91 ± 0.66	41.30 ± 0.39	0.06 ± 0.02
	2	40	2.54 ± 0.03	0.56 ± 0.05	46.65 ± 0.28	41.80 ± 0.65	0.12 ± 0.01
Bark	2	5	2.39 ± 0.05	0.45 ± 0.07	46.00 ± 0.66	41.89 ± 0.69	0.10 ± 0.02
	2	40	2.44 ± 0.08	0.68 ± 0.02	46.84 ± 0.48	40.49 ± 0.51	0.16 ± 0.00
	4	20	2.51 ± 0.13	0.37 ± 0.06	48.07 ± 0.50	45.03 ± 0.18	0.08 ± 0.01
	6	5	1.95 ± 0.05	0.10 ± 0.03	44.32 ± 1.40	43.29 ± 1.77	0.02 ± 0.01
Needles	2	5	2.29 ± 0.03	0.27 ± 0.02	42.84 ± 0.77	40.21 ± 1.02	0.06 ± 0.01
	6	5	2.33 ± 0.05	0.56 ± 0.05	47.93 ± 1.57	42.74 ± 1.93	0.12 ± 0.02
	6	40	2.41 ± 0.04	0.55 ± 0.04	46.45 ± 0.80	41.41 ± 0.52	0.12 ± 0.01

3.3 Flow performance

The fundamental design parameters crucial for a feed bin or hopper are the hopper orientation (*e.g.* inclination angle, which is the angle between the sloping side of the hopper and the vertical plane) and discharge opening. These parameters significantly influence the discharge rate through the cross-sectional opening and play a vital role in ensuring consistent material flow while preventing stress bridge formation (arching) that might hinder the gravitational flow of bulk solids [6, 25]. The data obtained from a wedge hopper for all the samples listed in Table S1 at various inclination angles is presented in Figure 3 and Table S2.

The results indicate that the critical arching distance, which refers to the minimum distance required for preventing arch formation, increases with the nominal particle size. For example, the critical arching distance for the 2 mm nominal particle size was approximately 13 mm, while it increased to 33 mm for the 6 mm nominal particle size at a 32° inclination angle. This suggests a greater propensity for particle interlock with larger particles [3]. The impact of inclination angle on the critical arching distance was generally minimal for most particle fractions, except for the needle-shaped particles. For instance, the critical arching distance measured 20.73 ± 2.12 mm and 25.03 ± 1.55 mm for the 2 mm size and 40% moisture content stem wood, respectively, at inclination angles of 28° and 36°. In contrast, the 2 mm size and 40% moisture content needles exhibited much higher critical arching distances of 38.70 ± 2.17 mm and 75.18 ± 6.62 mm at the same inclination angles.

Additionally, higher moisture content led to a slightly increased critical arching distance for smaller particle sizes, primarily due to the enhanced cohesion facilitated by moisture. However, this contribution of cohesion from moisture content became negligible for larger grind-sized materials. While the presence of a liquid bridge enhances cohesion in both particle sizes, this effect is amplified for smaller particles. When a limited amount of moisture is available, it tends to accumulate at the contact points between particles. The surface tension of the liquid induces the formation of a meniscus, resulting in negative capillary pressure within the liquid bridge. This pressure differential exerts an attractive force, drawing the particles closer together [45-47]. Biomass particles are typically irregular and porous, that facilitate the formation of liquid bridges and enhance the capillary effect. The surface area-to-volume ratio is greater for smaller particles, meaning that the surface-driven capillary forces have a greater influence relative to particle mass [48]. In contrast, larger particles are more significantly influenced by gravitational and inertial forces, the cohesive force from a liquid bridge is less significant; consequently, the effect of moisture on larger particles is negligible.

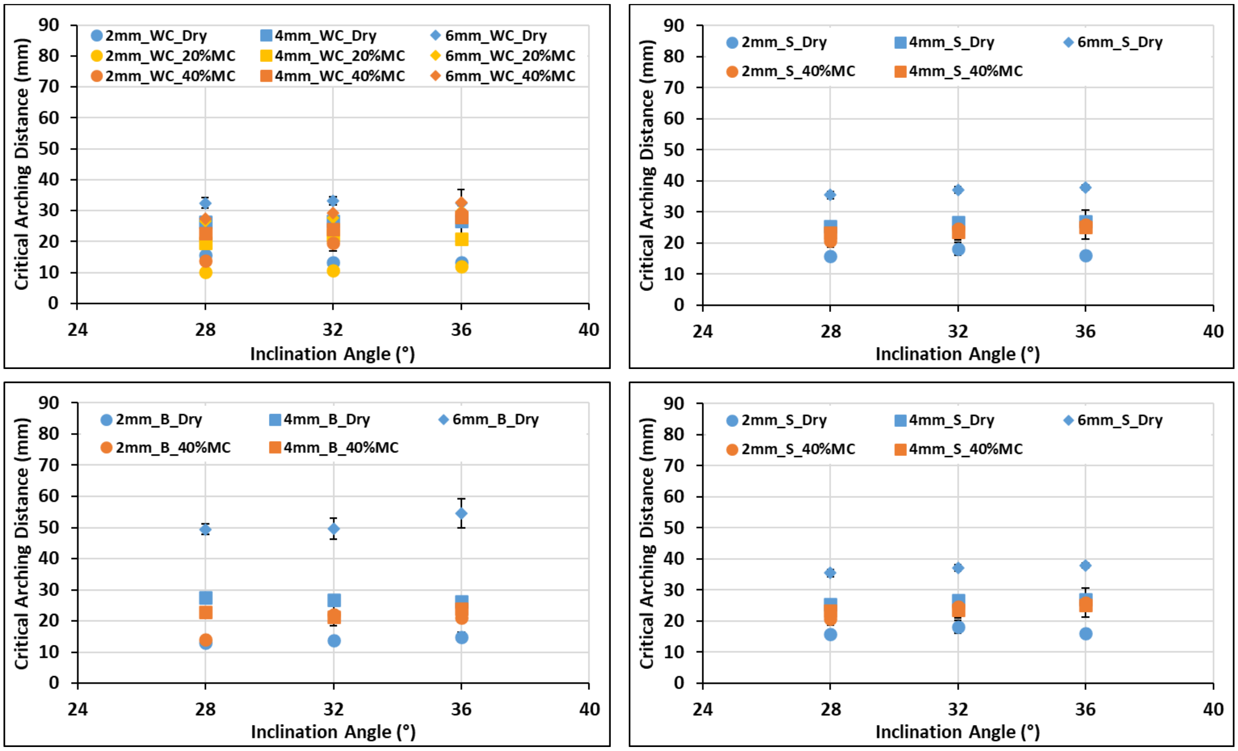

Figure 3: Critical arching distances of anatomical fractions, such as whole chips (top left), stem (top right), bark (bottom left), and needles (bottom right) in a wedge hopper.

When the hopper opening surpasses the critical arching distance, the loaded material can smoothly flow through the opening. However, if the opening is only slightly larger than the critical arching distance, the mass flow rate does not follow a linear relationship, as depicted in Figure S1, as well as past work [3]. To assess the discharge rate for each material and inclination angle accurately, the hopper was deliberately opened well beyond the critical arching distance to establish a continuous mass flow. Figure 4 and Figures S2-S5 present illustrative examples of flow behavior for various grind sizes, moisture contents, and anatomical fractions. Figure S2 demonstrates that the inclination angle has a minimal effect on the flow rate, whereas grind size exerts the most significant impact (see Figure S3). As particle size increases, the flowrate decreases at a given hopper opening. This observation may be attributed to lower packing density at the hopper discharge, resulting in reduced flow rates. The mass flowrate (considering a wet basis) shows an increase with a higher moisture content. However, when the flowrates are adjusted to a dry basis, a decreasing trend is observed (see Figure S4). This phenomenon was expected since moisture (water) possesses a higher mass per unit volume (density) compared to the studied materials, thereby influencing the mass flowrate calculations. The effect of moisture content on the mass flowrate followed a similar trend regardless of the particle size. The flow behavior of individual fractions, as depicted in Figure S5, indicates that whole chips and stems exhibit similar flow rates, while the needles exhibit the poorest flow rate among the fractions. This discrepancy in flow behavior can be attributed to the distinctive shape and characteristics of needle-shaped particles in comparison to the other anatomical fractions [50].

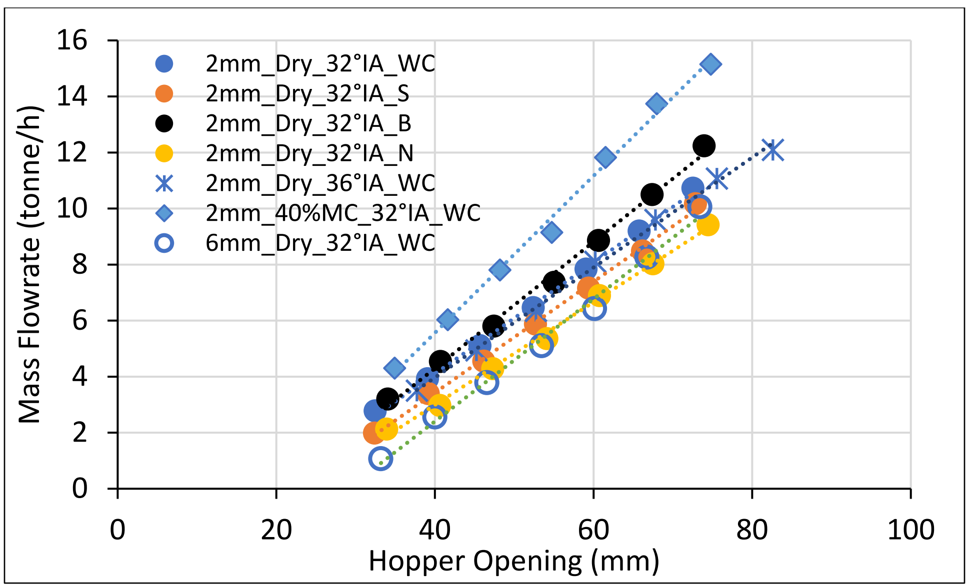

Figure 4: Flow performance of various anatomical fractions of loblolly pine at different moisture contents and hopper's inclination angels.

In comparison to the measured shear properties, there are a few key observations that can be made. Smaller particle sizes and higher moisture content generally increase cohesion and UYS, leading to higher critical arching distances and reduced flow rates. Conversely, larger particle sizes, which decrease cohesion, tend to have lower critical arching distances and higher flow rates. UYS represents the stress required to cause the material to fail in shear without confinement. Materials with higher UYS, such as bark and whole residues, are more resistant to flow initiation. This is particularly evident in the hopper experiments where materials with higher UYS exhibited greater critical arching distances and lower flow rates [43]. Cohesion, which can be influenced by particle size and moisture content as described above, plays a significant role in determining the critical arching distance and flow rates. Higher cohesion, due to either smaller particle sizes or higher moisture content, can increase the critical arching distance, thereby affecting the flowability of the material through the hopper. Finally, it is likely that the internal friction angle impacts the stability of the flow within the hopper. Higher internal friction angles, which are typically observed in materials with higher surface roughness and larger particle sizes, can lead to increased resistance to flow [40, 44]. This may result in reduced flow rates and higher critical arching distances.

3.4 Validate the design equations of wedge-shaped hopper

Figure 5, Figure S6, and Figure S7 present a comparison between the experimentally measured and model-predicted mass flow rates of different anatomical fractions. The results indicate that the ML model can predict the mass flow rate with relatively higher accuracy compared to the empirical model. However, the ML model does not exhibit as diverse predictions between materials or conditions as the previously established empirical model [6, 25]. It is important to note that the ML model was developed based on the physical characterization of whole pine materials. Given that different anatomical fractions, even from the same source, may exhibit significant differences in compressibility, shear resistance, particle density, and void ratios, variations in prediction accuracy for the anatomical fractions were anticipated.

The ML model predicted the flow rate of stem wood with reasonable accuracy, achieving a root mean square error (RMSE) of 0.37-0.53 tonne/h. This may be attributed to the stem wood being the most similar to the whole chips. Interestingly, the needles, which are physically and mechanically distinct from the whole chips, also showed good agreement with the predictions.

Due to the limitations of the hopper, experimental flow rates were only available for the 2 mm needles, which were then compared with the predicted flow rates. The physical and mechanical properties of the 2 mm needles were similar to those of the whole chips, whereas the larger sizes (4 mm and 6 mm) exhibited different properties. Therefore, it would be valuable to generate experimental flow rates for the 4 mm and 6 mm needles and compare them with the model predictions.

Conversely, the empirical model consistently overpredicted the mass flow rate for all anatomical fractions, regardless of the hopper operating conditions. There are several factors that explain this overestimation. Firstly, hammer-milled whole loblolly pine samples, which were used to calibrate the G-B model for FEM simulation, have a wider PSD than the samples produced by the shredder used in this study and the nominal particle size (*i.e.,* 2mm, 4mm, 6mm screen size) is larger than its true D_{50}. Secondly, FEM is a mesh-based method, and its numerical accuracy for large deformation is not as good as the meshless Lagrangian SPH model. Lastly, the empirical model was only fitted based on around 100 data points, while the ML model was trained and validated over 2000 data points. The empirical equation based on multiplication of exponent functions is not able to capture all the nonlinear relationship between inputs and output, while the multilayer perception can capture those subtle patterns with enough data.

With the above reasoning, we conclude that the empirical model as formulated only works for a narrow range of materials with properties similar to the hammer-milled loblolly pine it was calibrated with, while the ML model is more accurate for predicting general woody biomass materials. However, with the advancement of ML and physics-based simulation, improvement on the ML model should be carried out for robustness by training on an enriched data set distinguishing anatomical fractions (*e.g.,* adding PSD and particle aspect ratio to the input layer).

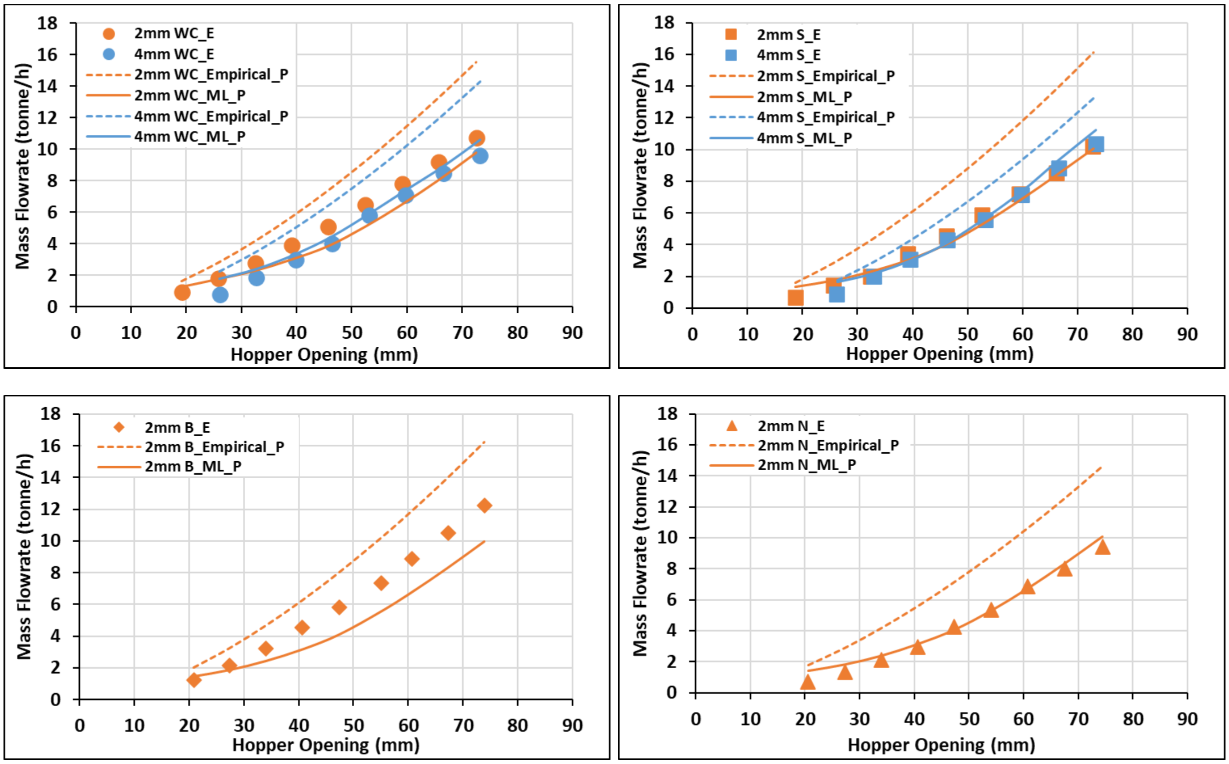

Figure 5: Experimental and predicted mass flowrate of various anatomical fractions at 32° inclination angle. The scattered points are the experimental (E) measurement where the dotted and solid lines represent the empirical and ML prediction (P), respectively.

The original formulation of the empirical flow equation was based on the particle density, critical state internal friction angle, dimensions of the hopper opening, and a term accounting for the mean particle size with a shape factor. To further develop this original formulation, there are several improvements that could be made to improve the mass flow rate prediction. As seen in the comparisons for both the flow results and shear properties, material shape and texture (surface roughness, particle angularity, etc.) are critical to differentiating results. It is likely that, because cohesion is predictable with information based on size and shape descriptors [44], reformulation of the shape factor could directly represent the apparent cohesion as well. Further to model additions, there was a strong dependance on feedstock moisture and both the shear properties as well as the hopper flow results, as documented in literature [51]. Finally, it is possible that the model would need to be parametrized to incorporate specific coefficients or factors for the different anatomical fractions (*i.e.,* whole chips, stem wood, bark, and needles) rather than be formulated with average parameter values. These coefficients should be based on experimental data that capture the unique flow behaviors of each fraction. Future work with controlled binary mixtures of biomasses/tissue fractions, followed by ternary mixtures, is needed to determine if these component interactions are linear and if a simple average is sufficient, or if more complex relationships are needed.

4 Conclusions

In conclusion, the comprehensive investigation into the flow behavior and shear properties of different anatomical fractions of loblolly pine including whole tree chips, and separated bark, clean white wood, and needs, reveals significant insights pertinent to optimizing biomass handling and processing systems. The study underscores the critical influence of particle size distribution, moisture content, and anatomical fraction on the physical and flow properties of biomass materials. The findings indicate that smaller particle sizes and higher moisture content generally lead to higher unconfined yield stress, and increased cohesion as measured in a Schulze ring shear tester, greater predicted and measured critical arching distances in wedge hoppers, resulting in negatively impacted flow rates. Conversely, larger particle sizes, which exhibit lower cohesion, tend to have lower critical arching distances, thereby facilitating improved flow rates. Regression equations developed previously to predict the flow of loblolly pine chips were compared to machine learning (ML) approaches using the collected ring shear test data and measured flow rates collected in this study. The experimental results, when compared with the previous empirical flow models, highlight the limitations of prior work that have not been developed for complex biomass mixtures such as forestry residues, and tend to overpredict mass flow rates for varied anatomical fractions. In contrast, the implemented ML approaches demonstrated higher predictive accuracy, although the method cannot directly account for specific material attributes, differences in anatomical fraction properties or portions of the various tissues, or process configuration.

Future research should focus on enhancing the ML approaches or the empirically developed regression equations by incorporating detailed descriptors of particle shape, texture, and specific coefficients for different anatomical fractions. Additionally, exploring the interactions in controlled mixtures of biomass fractions could provide deeper insights into the non-linear relationships affecting flow behaviors. Advancing the understanding and predictive capabilities in this area can significantly contribute to the efficient commercialization of biomass as a sustainable energy source.

Acknowledgements

The research was supported by the U.S. Department of Energy (DOE), Office of Energy Efficiency and Renewable Energy (EERE), Bioenergy Technologies Office (BETO), the Feedstock-Conversion Interface Consortium (FCIC), under DOE Idaho Operations Office with Contract No. DE-AC07-05ID14517.

References:

[1] Y. Liu, H. Lu, X. Guo, X. Gong, X. Sun, W. Zhao, An investigation of the effect of particle size on discharge behavior of pulverized coal, Powder Technology, 284 (2015) 47–56.

[2] N. Saha, C. Goates, S. Hernandez, W. Jin, T. Westover, J. Klinger, Characterization of particle size and moisture content effects on mechanical and feeding behavior of milled corn (Zea mays L.) stover, Powder Technology, 405 (2022) 117535.

[3] J. Klinger, N. Saha, T. Bhattacharjee, S. Carilli, W. Jin, Y. Xia, R. Daniel, C. Burns, O. Ajayi, Z. Cheng, Multiscale shear properties and flow performance of milled woody biomass, Frontiers in Energy Research, 10 (2022) 855289.

[4] Z. Cheng, J.H. Leal, C.E. Hartford, J.W. Carson, B.S. Donohoe, D.A. Craig, Y. Xia, R.C. Daniel, O.O. Ajayi, T.A. Semelsberger, Flow behavior characterization of biomass Feedstocks, Powder Technology, 387 (2021) 156–180.

[5] D. Ilic, K. Williams, R. Farnish, E. Webb, G. Liu, On the challenges facing the handling of solid biomass feedstocks, Biofuels, Bioproducts and Biorefining, 12 (2018) 187–202.

[6] T. Westover, D.S. Hartley, Biomass handling and feeding, Advances in biofuels and bioenergy, 86 (2018).

[7] N. Deak, H. Sitaraman, Y. Lu, N. Saha, J. Klinger, Y. Xia, A high-performance discrete-element framework for simulating flow and jamming of moisture bearing biomass feedstocks, Powder Technology, 452 (2025) 120548.

[8] R.M. Emerson, N. Saha, P.H. Burli, J.L. Klinger, T. Bhattacharjee, L. Vega-Montoto, Analyzing Potential Failures and Effects in a Pilot-Scale Biomass Preprocessing Facility for Improved Reliability, Energies, 17 (2024) 2516.

[9] N. Saha, J. Klinger, S.M. Rowland, T. Dunning, D. Carpenter, Z. Mills, J. Parks, Influence of feedstock variability on thermal decomposition of forest residue in a screw feeder for high temperature conversion, Fuel Processing Technology, 245 (2023) 107725.

[10] R.B. Shah, M.A. Tawakkul, M.A. Khan, Comparative evaluation of flow for pharmaceutical powders and granules, Aaps Pharmscitech, 9 (2008) 250–258.

[11] A. Vasilenko, B.J. Glasser, F.J. Muzzio, Shear and flow behavior of pharmaceutical blends—Method comparison study, Powder Technology, 208 (2011) 628–636.

[12] M. Benković, S. Srečec, I. Špoljarić, G. Mršić, I. Bauman, Flow properties of commonly used food powders and their mixtures, Food and bioprocess technology, 6 (2013) 2525–2537.

[13] V. Garg, S. Mallick, P. García-Trinanes, R.J. Berry, An investigation into the flowability of fine powders used in pharmaceutical industries, Powder technology, 336 (2018) 375–382.

[14] P. Juliano, B. Muhunthan, G.V. Barbosa-Cánovas, Flow and shear descriptors of preconsolidated food powders, Journal of food engineering, 72 (2006) 157–166.

[15] M.R. Wu, D.L. Schott, G. Lodewijks, Physical properties of solid biomass, Biomass and Bioenergy, 35 (2011) 2093–2105.

[16] A. Hamed, Y. Xia, N. Saha, J. Klinger, D.N. Lanning, J.H. Dooley, Particle size and shape effect of Crumbler® rotary shear-milled granular woody biomass on the performance of Acrison® screw feeder: A computational and experimental investigation, Powder Technology, 427 (2023) 118707.

[17] L.P. Matallana-Ramirez, R.W. Whetten, G.M. Sanchez, K.G. Payn, Breeding for climate change resilience: a case study of loblolly pine (Pinus taeda L.) in North America, Frontiers in plant science, 12 (2021) 606908.

[18] S.E. McKeand, K.G. Payn, A.J. Heine, R.C. Abt, Economic significance of continued improvement of loblolly pine genetics and its efficient deployment to landowners in the southern United States, Journal of Forestry, 119 (2021) 62–72.
[19] R. Navar, J.H. Leal, B.L. Davis, T.A. Semelsberger, Rheological effects of moisture content on the anatomical fractions of loblolly pine (Pinus taeda), Powder Technology, 412 (2022) 118031.
[20] K. Pardikar, C. Wassgren, Predicting the critical outlet width of a hopper using a continuum finite element method model, Powder Technology, 356 (2019) 649–660.
[21] A. Drescher, A. Waters, C. Rhoades, Arching in hoppers: II. Arching theories and critical outlet size, Powder Technology, 84 (1995) 177–183.
[22] J. Xue, S. Schiano, W. Zhong, L. Chen, C.-Y. Wu, Determination of the flow/no-flow transition from a flat bottom hopper, Powder Technology, 358 (2019) 55–61.
[23] J. Guo, A.W. Roberts, J.-D. Prigge, Experimental investigation of wall pressure and arching behavior under surcharge pressure in mass-flow hoppers, Powder technology, 258 (2014) 272–284.
[24] S.V. Søgaard, N.E. Olesen, C. Hirschberg, M.H. Madsen, M. Allesø, J. Garnaes, J. Rantanen, An experimental evaluation of powder flow predictions in small-scale process equipment based on Jenike's hopper design methodology, Powder technology, 321 (2017) 523–532.
[25] Y. Lu, W. Jin, J. Klinger, S. Dai, Flow and arching of biomass particles in wedge-shaped hoppers, ACS Sustainable Chemistry & Engineering, 9 (2021) 15303–15314.
[26] Y. Lu, W. Jin, N. Saha, J.L. Klinger, Y. Xia, S. Dai, Wedge-Shaped Hopper Design for Milled Woody Biomass Flow, ACS Sustainable Chemistry & Engineering, 10 (2022) 16803–16813.
[27] A. Ikbarieh, W. Jin, Y. Zhao, N. Saha, J.L. Klinger, Y. Xia, S. Dai, Machine Learning Assisted Cross-Scale Hopper Design for Flowing Biomass Granular Materials, ACS Sustainable Chemistry & Engineering, (2025).
[28] A.S.S. 2, Moisture Measurement–Forages, American Society of Agricultural and Biological Engineers St. Joseph, MI, 2006.
[29] A.S. ANSI, ASAE S319. 3 FEB03, Method of determining and expressing fineness of feed materials by sieving.
[30] S. ASAE, S269. 4-Cubes, Pellets, and Crumbles–Definitions and Methods for Determining Density, Durability, and Moisture Content ASAE DEC, 96.
[31] C.E. Brewer, V.J. Chuang, C.A. Masiello, H. Gonnermann, X. Gao, B. Dugan, L.E. Driver, P. Panzacchi, K. Zygourakis, C.A. Davies, New approaches to measuring biochar density and porosity, Biomass and Bioenergy, 66 (2014) 176–185.
[32] R.M. Nedderman, Statics and kinematics of granular materials, (No Title), (1992).
[33] D. Schulze, Powders and bulk solids, Springer2021.
[34] Y. Lu, W. Jin, J. Klinger, T.L. Westover, S. Dai, Flow characterization of compressible biomass particles using multiscale experiments and a hypoplastic model, Powder Technology, 383 (2021) 396–409.
[35] R. Zamora-Cristales, J. Sessions, D. Smith, G. Marrs, Effect of grinder configuration on forest biomass bulk density, particle size distribution and fuel consumption, Biomass and Bioenergy, 81 (2015) 44–54.
[36] J. Zhu, C.T. Scott, K.L. Scallon, G.C. Myers, Effects of plantation density on wood density and anatomical properties of red pine (Pinus resinosa Ait.), Wood and fiber science. Vol. 39, no. 3 (2007): pages 502-512., (2007).

[37] C. Fernandes, M.J. Gaspar, J. Pires, A. Alves, R. Simões, J.C. Rodrigues, M.E. Silva, A. Carvalho, J.E. Brito, J.L. Lousada, Physical, chemical and mechanical properties of Pinus sylvestris wood at five sites in Portugal, IForest, (2017).
[38] M. Stasiak, M. Molenda, M. Gancarz, J. Wiącek, P. Parafiniuk, A. Lisowski, Characterization of shear behaviour in consolidated granular biomass, Powder Technology, 327 (2018) 120–127.
[39] M. Stasiak, M. Molenda, M. Bańda, J. Horabik, J. Wiącek, P. Parafiniuk, J. Wajs, M. Gancarz, E. Gondek, A. Lisowski, Friction and shear properties of pine biomass and pellets, Materials, 13 (2020) 3567.
[40] S. Hernandez, T.L. Westover, A.C. Matthews, J.C.B. Ryan, C.L. Williams, Feeding properties and behavior of hammer-and knife-milled pine, Powder technology, 320 (2017) 191–201.
[41] N. Saha, J. Klinger, T. Bhattacharjee, N. Berglund, W. Jin, Y. Xia, Effect of Particle Size, Moisture Content, and Tissue Fraction on Mechanical and Feeding Behavior of Milled Corn Stover and Loblolly Pine Residues, 2023 AIChE Annual Meeting, 2023.
[42] L. Krátký, Mechanical size reduction of lignocellulosic biomass: a mini-review, Chemical Engineering Transactions, 94 (2022) 229–234.
[43] M. Przywara, R. Lech-Przywara, W. Zapała, I. Opaliński, Mechanical properties of solid biomass as affected by moisture content, AgriEngineering, 5 (2023).
[44] T. Bhattacharjee, J. Klinger, E. Fillerup, S. Carilli, M.S. Casajus, W. Jin, Y. Xia, Effects of particle size, distribution, and morphology on bulk shear behavior of milled loblolly pine, Powder Technology, 457 (2025) 120911.
[45] K. Johanson, Y. Rabinovich, B. Moudgil, K. Breece, H. Taylor, Relationship between particle scale capillary forces and bulk unconfined yield strength, Powder Technology, 138 (2003) 13–17.
[46] N. Harnby, Chapter 5 - The mixing of cohesive powders, in: N. Harnby, M.F. Edwards, A.W. Nienow (Eds.) Mixing in the Process Industries, Butterworth-Heinemann, Oxford, 1992, pp. 79–98.
[47] H.N.G. Nguyen, C.-F. Zhao, O. Millet, A.P.S. Selvadurai, Effects of surface roughness on liquid bridge capillarity and droplet wetting, Powder Technology, 378 (2021) 487–496.
[48] E. Koos, Capillary suspensions: Particle networks formed through the capillary force, Current Opinion in Colloid & Interface Science, 19 (2014) 575–584.
[49] BE&E, Understanding Moisture's Impact on Biomass Handling.
[50] Q. Gou, X. Wang, G. Chen, S. Liu, Effect of particle shape on particle flow and heat transfer behavior based on computational fluid dynamics-discrete element modeling, Physics of Fluids, 37 (2025).
[51] Y. Lu, W. Jin, J.L. Klinger, S. Dai, Effects of the Moisture Content on the Flow Behavior of Milled Woody Biomass, ACS Sustainable Chemistry & Engineering, (2023).